

# The first electron beam polarization measurement with a diamond micro-strip detector

A. Narayan<sup>1</sup>, D. Dutta<sup>1</sup>, V. Tvaskis<sup>2,3</sup>, D. Gaskell<sup>4</sup>, J. W. Martin<sup>2</sup>, A. Asaturyan<sup>5</sup>, J. Benesch<sup>4</sup>, G. Cates<sup>6</sup>, B. S. Cavness<sup>7</sup>, J. C. Cornejo<sup>8</sup>, M. Dalton<sup>6</sup>, W. Deconinck<sup>8</sup>, L. A. Dillon-Townes<sup>4</sup>, G. Hays<sup>4</sup>, E. Ihloff<sup>9</sup>, D. Jones<sup>6</sup>, R. Jones<sup>10</sup>, S. Kowalski<sup>11</sup>, L. Kurchaninov<sup>12</sup>, L. Lee<sup>12</sup>, A. McCreary<sup>13</sup>, M. McDonald<sup>2</sup>, A. Micherdzinska<sup>2</sup>, A. Mkrтчyan<sup>5</sup>, H. Mkrтчyan<sup>5</sup>, V. Nelyubin<sup>6</sup>, S. Page<sup>3</sup>, K. Paschke<sup>6</sup>, W. D. Ramsay<sup>12</sup>, P. Solvignon<sup>4</sup>, D. Storey<sup>2</sup>, A. Tobias<sup>6</sup>, E. Urban<sup>14</sup>, C. Vidal<sup>9</sup>, P. Wang<sup>3</sup>, and S. Zhamkotchyan<sup>5</sup>

<sup>1</sup>Mississippi State University, Mississippi State, MS 39762, USA

<sup>2</sup>University of Winnipeg, Winnipeg, MB R3B 2E9, Canada

<sup>3</sup>University of Manitoba, Winnipeg, MB R3T 2N2, Canada

<sup>4</sup>Thomas Jefferson National Accelerator Facility, Newport News, VA 23606, USA

<sup>5</sup>Yerevan Physics Institute, Yerevan, 375036, Armenia

<sup>6</sup>University of Virginia, Charlottesville, VA 22904, USA

<sup>7</sup>Angelo State University, San Angelo, TX 76903, USA

<sup>8</sup>College of William and Mary, Williamsburg, VA 23186, USA

<sup>9</sup>MIT Bates Linear Accelerator Center, Middleton, MA 01949, USA

<sup>10</sup>University of Connecticut, Storrs, CT 06269, USA

<sup>11</sup>Massachusetts Institute of Technology, Cambridge, MA 02139, USA

<sup>12</sup>TRIUMF, Vancouver, BC V6T 2A3, Canada

<sup>13</sup>University of Pittsburgh, Pittsburgh, PA 15260, USA and

<sup>14</sup>Hendrix College, Conway, AR 72032, USA

A diamond multi-strip detector was used for the first time, to track Compton scattered electrons in a new electron beam polarimeter in experimental Hall C at Jefferson Lab. We report the first polarimetry results with electrons detected in diamond multi-strip detectors. The analysis technique leveraged the high resolution of the detectors and their proximity to the electron beam ( $\gtrsim 0.5$  cm). For a 1.16 GeV electron beam with currents up to 180  $\mu$ A the beam polarization was measured with a statistical precision of  $< 1\%$ /hr. The systematic uncertainty due to the electron detector was 0.56%. This constitutes the first demonstration of high precision polarimetry with diamond based detectors.

PACS numbers:

## INTRODUCTION

High precision nuclear physics experiments using polarized electron beams rely on accurate knowledge of beam polarization to achieve their ever improving precision. A parity violating electron scattering (PVES) experiment in the experimental Hall C at Jefferson Lab (JLab), known as the  $Q_{\text{weak}}$  experiment, is the most recent example [1, 2]. The goal of the  $Q_{\text{weak}}$  experiment is to measure the Standard Model parameter known as the weak mixing angle, at a low energy (relative to the  $Z^0$  mass) with unprecedented precision. With a goal of  $< 1\%$  uncertainty, determination of electron beam polarization is one of the greatest technical challenges of the  $Q_{\text{weak}}$  experiment. The experiment utilized an existing Møller polarimeter [2, 3] and a new Compton polarimeter [2, 4] to monitor the electron beam polarization. The Compton polarimeter was the only polarimeter at JLab Hall C that could non-destructively monitor the beam polarization at very high beam currents. A novel aspect of this polarimeter was the first use of diamond detector technology for this purpose.

The use of *natural* diamond in the detection of charged particles and radiation has a long history; but the use of

synthetic diamond grown through a process known as “chemical vapor deposition” (CVD) is a relatively recent development. Detailed reviews of diamond as charged particle detectors can be found in [11–13]. Thin sheets of centimeter-sized diamond are grown using the CVD process and the plates of diamond are then turned into charged particle detectors by depositing suitable electrodes on them [14]. Compared to the more commonly used silicon detector, the signal size in a diamond detector is smaller, but the higher electron and hole mobility of diamond leads to a faster and shorter duration signal. However, the well-established radiation hardness of diamond [15, 16] is by far the most important consideration for the use of diamond detectors in nuclear and particle physics experiments.

The use of Compton scattered electrons and/or back-scattered photons to measure the Compton asymmetry and thereby the electron beam polarization, is a well established polarimetry technique [5–10]. Most previous Compton polarimeters, other than the one used in the SLD experiment [7], relied primarily on detection of the scattered photons to measure the beam polarization. The SLD Compton polarimeter, which detected scattered electrons (and used detection of photons as a

cross-check), was operated at a beam energy of 50 GeV.<sup>101</sup> The low energy of the electron beam (1.16 GeV) and<sup>102</sup> other operating parameters of the  $Q_{\text{weak}}$  experiment, pre-<sup>103</sup> sented the most challenging set of conditions for precision<sup>104</sup> beam polarimetry. For example, it constrained the track-<sup>105</sup> ing detector to be placed as close as 0.5 cm from the<sup>106</sup> electron beam. Further, the polarimeter was operated<sup>107</sup> at the highest beam current (180  $\mu\text{A}$ ) ever used by any experiment at JLab and ran for over 5000 hrs, thereby subjecting the electron detectors to a rather large cumulative radiation dose ( $> 100$  kGy, just from electrons). In order to withstand the large radiation dose, a novel set of diamond micro-strip detectors were used to track the scattered electrons in the JLab Hall C Compton polarimeter. In this letter we report the first measurement of electron beam polarization with this device.

## THE HALL C COMPTON POLARIMETER

The Compton polarimeter in Hall C at JLab is described in Ref. [2, 4]. The Compton scattered electrons were momentum analyzed by a dipole magnet which bent the primary beam by  $\sim 10.13^\circ$ . The maximum separation between the primary electron beam and the Compton scattered electrons, at the location of the electron detector, was  $\sim 17$  mm. The deflection of the scattered electrons with respect to the primary electron beam, from the maximum down to distances as small as  $\sim 5$  mm, was tracked by a set of four diamond micro-strip detectors.<sup>108</sup> This range allowed the detection of a large fraction of the Compton electron spectrum, from beyond the kinematic maximum (strip 55 in Fig. 2) down past the zero-crossing point ( $\sim 8.5$  mm from the primary beam) of the Compton asymmetry. The electron detectors were made from 21 mm $\times$ 21 mm $\times$ 0.5 mm plates of CVD diamond [2]. Each diamond plate has 96 horizontal metalized electrode strips with a pitch of 200  $\mu\text{m}$  (180  $\mu\text{m}$  of metal and 20  $\mu\text{m}$  of gap) on one side. Further details can be found in Ref. [2, 4]. A photograph of a single detector plane is shown in Fig 1.

A Compton electron rate, aggregated over all strips in each detector plane, of  $\sim 150$ – $180$  kHz was observed with these detectors and the signal-to-background ratio was  $\sim 5$ – $20$  [2]. By comparing the expected to the observed rates, the detector efficiency was estimated to be  $\sim 70\%$ . The large separation between the detector and the readout electronics was the leading cause of the inefficiency.

The data acquisition (DAQ) system employed a set of field programmable gate array (FPGA) based logic modules to find clusters of detector hits, and to implement a track-finding algorithm, which generated a trigger when the same cluster was identified in multiple active planes. The cluster size was set to 4 adjacent strips. Only 3 detector planes were operational during the experiment and

the typical trigger condition was set to 2 out of 3 planes.

Over the 2 year period of the  $Q_{\text{weak}}$  experiment, the detectors were exposed to a radiation dose of  $\sim 100$  kGy (without including the dose from Synchrotron radiation). No significant degradation of the signal size was observed during this period, demonstrating the radiation hardness of the diamond detectors.

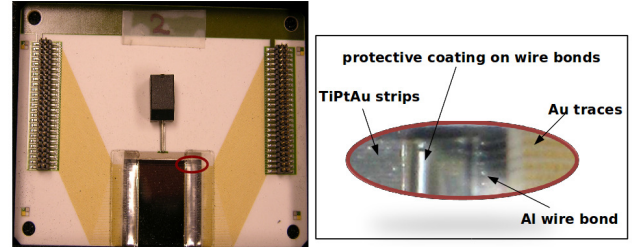


FIG. 1: A CVD diamond plate mounted on an alumina substrate which forms a single detector plane (left). The red oval indicates the area that has been shown in the enlarged view (right).

## DATA REDUCTION AND RESULTS

The electron beam helicity was reversed at a rate of 960 Hz in a pseudo-random sequence. In addition a half-wave plate in the polarized electron photo emission source [17] was inserted or removed about every 8 hours to reverse the beam helicity relative to the polarization of the source laser.

The Compton laser was operated in  $\sim 90$  second cycles ( $\sim 60$  s on and  $\sim 30$  s off). The laser off data were used to measure the background. The background yield measured during the laser-off period was subtracted from the laser-on yield for each electron helicity state, and a charge normalized Compton yield for each detector strip was obtained for the two electron helicities. The measured asymmetry was built from these yields using,

$$A_{exp} = \frac{Y^+ - Y^-}{Y^+ + Y^-}, \quad (1)$$

where  $Y^\pm = \frac{N_{on}^\pm}{Q_{on}^\pm} - \frac{N_{off}^\pm}{Q_{off}^\pm}$  is the charge normalized Compton yield for each detector strip,  $N_{on/off}^\pm$  and  $Q_{on/off}^\pm$  are the detector counts and the beam charge accumulated during the laser on/off period for the two electron helicity states ( $\pm$ ), respectively. A statistical precision of  $< 1\%$  per hour was routinely achieved. The Compton yields were integrated over two different time intervals,  $\sim 250$  thousand helicity cycles and 1 laser cycle. The asymmetries extracted over both time intervals, and averaged over an hour long run, were consistent with one another. A typical spectrum for an hour long run is shown

134 in Fig. 2. The background asymmetry is consistent with  
 135 zero within the statistical uncertainties, and given the  
 136 large signal-to-background ratio of 5–20, the dilution to  
 137 the measured asymmetry due to the background is neg-  
 138 ligible.

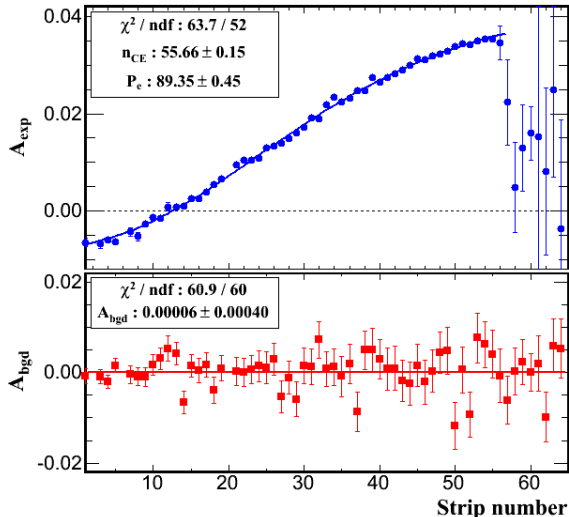


FIG. 2: The measured asymmetry as function of detector strip number for a single detector plane during the laser-on period (top) and the background asymmetry from the laser-off period (bottom). The strip number is linearly mapped to the displacement of the scattered electron from the primary beam. The solid blue line (top) is a fit to Eq. 2 and the solid red line (bottom) is a fit to a constant value. Only statistical uncertainties are shown in this figure.

139 The electron beam polarization  $P_e$  was extracted by  
 140 fitting the measured asymmetry to the theoretical Com-  
 141 ton asymmetry using;

$$A_{exp}(y_n) = P_e P_\gamma A_{th}(y_n), \quad (2)$$

142 where  $P_\gamma$  is the polarization of the photon beam,  $y_n$  is the  
 143 scattered electron displacement along the detector plane  
 144 for the  $n$ -th strip, and  $A_{th}$  is the  $\mathcal{O}(\alpha)$  theoretical Com-  
 145 ton asymmetry for fully polarized electrons and photon  
 146 beams. The radiative corrections to the Compton asym-  
 147 metry were calculated to leading order within a low en-  
 148 ergy approximation applicable for few GeV electrons [18].  
 149 The relative change in the Compton asymmetry due to  
 150 radiative corrections was  $<0.3\%$ .

151 The quantity  $A_{th}$  is typically calculated as a function of  
 152 the dimensionless variable  $\rho = E_\gamma/E_\gamma^{max}$ , where  $E_\gamma$  and  
 153  $E_\gamma^{max}$  are the energy of the back-scattered photon and its  
 154 maximum value, respectively. In order to directly com-  
 155 pare with the measured asymmetry,  $\rho$  was mapped, by a  
 156 third order polynomial, to the displacement of the scat-  
 157 tered electron along the detector plane  $y_n$ . Further,  $y_n$  is  
 158 linearly related to detector strip number, and depends on  
 159 several parameters, such as, dimensions and dispersion of

the chicane magnets, and exact location of the detectors with respect to the third dipole.

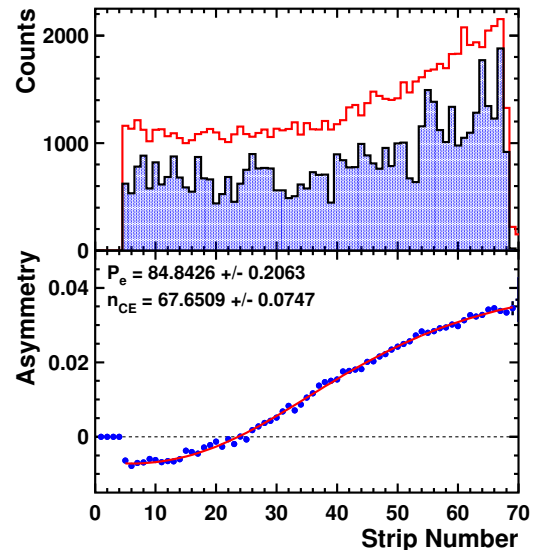


FIG. 3: (top) A typical Monte Carlo simulated Compton spectrum for a single detector plane, with (blue, shaded) and without (red) detector inefficiency. The counts have been scaled by a factor of  $10^{-3}$ . (bottom) The Compton asymmetry extracted from the simulated spectrum including detector inefficiency (blue circles), and a two parameter fit to the calculated asymmetry (red line). The input asymmetry was 85%.

162 The measured asymmetry  $A_{exp}$  was fit to Eq. 2 for  
 163 each detector strip, with  $P_e$  and  $n_{CE}$  (the strip number  
 164 that detects the maximum displaced electrons) as the two  
 165 free parameters. The number of degrees of freedom was  
 166 typically between 50 – 60, which was made possible by  
 167 the high resolution of the detector, and the proximity of  
 168 the detector to the primary electron beam. The detection  
 169 of a large fraction of the Compton electron spectrum,  
 170 spanning both sides of the zero crossing of the Compton  
 171 asymmetry, significantly improved the robustness of the  
 172 fit and the analysis technique. A typical fit is shown in  
 173 Fig. 2. The  $\chi^2$  per degree-of-freedom of the fit ranges  
 174 between 0.8 – 1.5 for all production runs reported here.

175 A Monte Carlo (MC) simulation of the Compton polar-  
 176 imeter was coded in the GEANT3 [19] detector simu-  
 177 lation package. In addition to Compton scattering, the  
 178 simulation included backgrounds from beam-gas inter-  
 179 actions and beam halo interactions in the chicane ele-  
 180 ments. The simulation also incorporated the effects of  
 181 detector inefficiency, the track-finding trigger, and elec-  
 182 tronic noise. A typical simulated strip-hit spectrum (with  
 183 and without detector inefficiency), and the asymmetry  
 184 extracted from simulated spectra are shown in Fig. 3.  
 185 The simulation was used to validate the analysis pro-  
 186 cedure and to study a variety of sources of systematic  
 187 uncertainty. For each source, the relevant parameter was

188 varied within the expected range of uncertainty, and the 223  
 189 change in the extracted polarization was listed as its con-224  
 190 tribution to the systematic uncertainty. The list of con-225  
 191 tributions is shown in Table I. 226

192 The MC simulation demonstrated that secondary par-227  
 193 ticles knocked out by the Compton scattered electron228  
 194 passing through the first plane produced a 0.4% change229  
 195 in polarization in the subsequent planes, consistent with230  
 196 observation. A correction for the second and third planes231  
 197 could be made but at the cost of a slightly higher sys-  
 198 tematic uncertainty, and hence only the results from the  
 199 first detector plane are quoted here.

200 There were several sources of inefficiency associated  
 201 with the DAQ system, such as the algorithm used to iden-  
 202 tify electron tracks and form the trigger, and the dead-  
 203 time due to a busy (hold off) period in the DAQ. The  
 204 entire DAQ system was simulated on a platform called  
 205 Modelsim [20]. While in Monte Carlo simulations, events  
 206 are generated based on the probability distribution for  
 207 the relevant physics process, in contrast Modelsim is a  
 208 simulation technique based on time steps. It employs  
 209 the same firmware, written in the hardware description  
 210 language for very high speed integrated circuits (VHDL),  
 211 that operated the logic modules in the DAQ system. The  
 212 DAQ simulation included signal generators that mimic  
 213 the electron, the background and the noise signals, along  
 214 with a detailed accounting of delays due to the internal  
 215 signal pathways in the logic modules and the external  
 216 electronic chain.

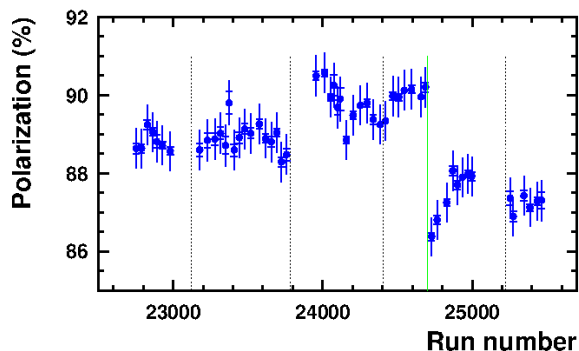


FIG. 4: The extracted beam polarization as a function of run-  
 number averaged over 30 hour long periods, during the second  
 run period of the  $Q_{weak}$  experiment. The inner error bars  
 show the statistical uncertainty while the outer error bar is  
 the quadrature sum of the statistical and the total systematic  
 uncertainties due the electron detector. The dashed and solid  
 (green) vertical lines indicate changes at the electron source.

217 The difference between the triggered and the un-  
 218 triggered counts observed in the DAQ simulation was245  
 219 due to DAQ inefficiency. Also, the average DAQ inef-246  
 220 ficiency was found to be directly related to the aggregate247  
 221 detector rate. These results were used to determine the248  
 222 correction to the detector yield for each 1 hr run, based249

on the aggregate detector rate during the run. The DAQ  
 inefficiency correction resulted in  $< 1\%$  change in the ex-  
 tracted polarization. The validity of the corrections and  
 the systematic uncertainty due to the corrections (listed  
 in Table I) was determined by comparing the polariza-  
 tion extracted from triggered vs. un-triggered data over  
 a wide range of beam currents (rates) and several differ-  
 ent trigger conditions. Thus, the Modelsim simulation  
 provided a robust method to determine the inefficiency  
 of the DAQ.

TABLE I: Systematic uncertainties of the electron detector

Source	Uncertainty	$\Delta P/P\%$
magnetic field	0.0011 T	0.13
beam energy	1 MeV	0.08
detector z position	1 mm	0.03
inter plane trigger	1-3 plane	0.19
trigger clustering	1-8 strips	0.01
detector tilt(w.r.t x, y and z)	1 degree	0.06
detector efficiency	0.0 - 1.0	0.1
detector noise	up to 20% of rate	0.1
fringe field	100%	0.05
radiative corrections	20%	0.05
DAQ inefficiency correction	40%	0.3
DAQ inefficiency pt.-to-pt.		0.3
Beam vert. pos. variation	0.5 mrad	0.2
helicity correl. beam pos.	5 nm	$< 0.05$
helicity correl. beam angle	3 nrad	$< 0.05$
spin precession in chicane	20 mrad	$< 0.03$
Total		0.56

232 Extensive simulation studies provided the comprehen-  
 233 sive list of contributions to the systematic uncertainties,  
 234 tabulated in Table I, with a net systematic uncertainty  
 235 of 0.56% for the electron detector. For the entire sec-  
 236 ond running period of the  $Q_{weak}$  experiment a statistical  
 237 precision of  $< 1\%/hr$  was routinely achieved. The po-  
 238 larization measured by the diamond detectors, as shown  
 239 in Fig. 4, was stable except for variations due changes  
 240 in the electron source. The measured polarization was con-  
 241 sistent with the Møller measurements [2–4] within the  
 242 experimental uncertainties of the two polarimeters.

## CONCLUSIONS

244 The polarization of a 1.16 GeV electron beam was mea-  
 245 sured using a set of diamond micro-strip detectors for the  
 246 first time. The high resolution of the detectors and their  
 247 proximity to the primary beam helped record a large frac-  
 248 tion of the Compton electron spectrum, spanning both

sides of the zero crossing of the Compton asymmetry.<sup>275</sup>  
 These detectors, coupled with a robust analysis technique<sup>276</sup>  
 and rigorous simulations of the polarimeter and the DAQ<sup>277</sup>  
 system, produced a very reliable, high precision measure-<sup>278</sup>  
 ment of the polarization in a very high radiation environ-<sup>279</sup>  
 ment. They demonstrate that diamond micro-strip de-<sup>280</sup>  
 tectors are indeed a viable option as tracking detectors,<sup>281</sup>  
 and they are the superior choice for tracking detectors<sup>282</sup>  
 that are exposed to very high radiation dose, such as<sup>283</sup>  
 electron detectors in Compton polarimeters operated at<sup>284</sup>  
 few-GeV beam energies.<sup>285</sup>

## ACKNOWLEDGMENTS

This work was funded in part by the U.S. Department<sup>292</sup>  
 of Energy contract # AC05-06OR23177, under which<sup>293</sup>  
 Jefferson Science Associates, LLC operates Thomas Jef-<sup>294</sup>  
 ferson National Accelerator Facility, and contract # DE-<sup>295</sup>  
 FG02-07ER41528, and by the Natural Sciences and Engi-<sup>296</sup>  
 neering Research Council of Canada (NSERC). We thank<sup>297</sup>  
 H. Kagan from Ohio State University for teaching us<sup>298</sup>  
 about diamonds, training us on characterizing them and<sup>299</sup>  
 helping us build the proto-type detector.<sup>300</sup>

- 
- [1] D. Androic *et al.*, Phys. Rev. Lett. **111**, 121804 (2013).<sup>306</sup>  
 [2] T. Allison *et al.*, Nucl. Instr. Meth. **A781**,105 (2015).<sup>307</sup>  
 [3] M. Hauger, A. Honegger, J. Jourdan, G. Kubon, T. Pe-  
 titjean, D. Rohe, I. Sick and G. Warren *et al.*, Nucl. In-

- strum. Meth. A **462**, 382 (2001); J. Magee, Proc. of Sci. PSTP2013, 039 (2013).  
 [4] A. Narayan, Ph. D. Thesis, Mississippi State University, 2015 (unpublished).  
 [5] D. Gustavson *et al.* Nucl. Instr. Meth. **A165**, 177 (1979); L. Knudsen *et al.*, Phys. Lett. **B270**, 97 (1991).  
 [6] D. P. Barber *et al.*, Nucl. Instr. Meth. **A329**, 79 (1993).  
 [7] M. Woods, Proc. of the Workshop on High Energy Polarimeters, Amsterdam, eds. C. W. de Jager *et al.*, p. 843 (1996); SLAC-PUB-7319 (1996).  
 [8] I. Passchier *et al.*, Nucl. Instr. Meth. **A414**, 446 (1998).  
 [9] W. Franklin *et al.*, AIP Conf.Proc. 675, 1058 (2003).  
 [10] M. Baylac *et al.*, Phys. Lett. **B539**, 8 (2002); N. Felletto *et al.*, Nucl. Instr. Meth. **A459**, 412 (2001).  
 [11] D. R. Kania, M. I. Landstrass and M. A. Plano, Diam. Relat. Mater. **2**, 1012 (1993).  
 [12] R. Berman (ed), *Physical Properties of Diamond*, Oxford University Press, Oxford, 1965.  
 [13] J. E. Field (ed), *The Properties of Diamond*, Academic, New York, 1979.  
 [14] R. J. Tapper, Rep. Prog. Phys. **63**, 1273 (2000).  
 [15] C. Bauer *et al.* Nucl. Instrum. Methods **367**, 207 (1995).  
 [16] M. M. Zoeller *et al.*, IEEE Trans. Nucl. Sci. **44** 815 (1997).  
 [17] C.K. Sinclair *et al.*, Phys. Rev. ST Accel. Beams **10**, 023501 (2007); P.A. Adderley *et al.*, Phys. Rev. ST Accel. Beams **13**, 010101 (2010).  
 [18] A. Denner and S. Dittmaier, Nucl. Phys.**B540**, 58 (1999).  
 [19] CERN Program Library Long Write-up W5013, Unpublished (1993)  
 [20] Modelsim Reference Manual, Mentor Graphics Corp., Unpublished (2010).